scientific reports

Check for updates

OPEN

A relationship between two-dimensional and four-dimensional space-time by comparing generalized two-dimensional Yang–Mills theory and Maxwell construction

Leila Lavaei

Some important problems in science do not have analytical solutions in four dimensions including *QCD*, but they are integrable in two dimensions. For many years, scientists have been trying to find a relation between two-dimensional and four-dimensional space-time to explain the real problem in four dimensions by accurately solving the appropriate model in two dimensions. In this paper, an interesting relation between gYM_2 (generalized two-dimensional Yang–Mills) and Maxwell construction has been found, which can be a starting point for finding more relations between two-dimensional and four-dimensional space-time, so this paper can play an important role in the advancement of science. For this purpose, first, the large-N behavior of the quartic-cubic generalized two-dimensional Yang–Mills $U(N)$ on a sphere is investigated for finite cubic couplings. It is shown that there are two phase transitions one of which is of third order, which is similar to previous papers, and the other one is of second order, which is a novel result. Second, gYM_2 (for $G(z) = z^m + \lambda z^n$; $m = 4, 6$; $n < m$) and Maxwell construction are compared with each other and a relationship between two-dimensional space-time, which is integrable, and four-dimensional space-time is obtained.

The YM_2 theory is defined by the lagrangian $tr(F^2)$ on a compact Riemann surface, where F is the 2-form field strength. If one considers $i\,tr(BF) + tr(B^2)$ as the Lagrangian of this theory, where B is an auxiliary pseudo-scalar field in the adjoint representation of the gauge group, and uses path-integral method over the field B, an effective Lagrangian of the form $tr(F^2)$ is concluded.

Because of two reasons, it is interesting that YM_2 theory be generalized. First, invariance under area-preserving diffeomorphisms and the lack of propagating degrees of freedom are two important properties of YM_2 that are not exclusive to the $i\,tr(BF) + tr(B^2)$ Lagrangian, but one can generalize this theory without losing these two properties. These generalized theories (gYM_2s) are defined by replacing the $tr(B^2)$ term by an arbitrary class function $f(B)$[1]. Second, it is conceivable that one of the generalized 2D models will reveal features which are more relevant and more closely resemble the four-dimensional theories of interest.

Two-dimensional Yang–Mills theory (YM_2) and generalized Yang–Mills theories (gYM_2s) have been a subject of extensive study[1–28]. They are important theories because they are integrable. It has been seen that there are certain relations between these theories and string theories. These relations can be seen by studying the large-N behavior of YM_2 (or gYM_2) based on $SU(N)$ that is shown in Refs.[13,16,17,19]. On the other hand, these theories can shed light on some basic features of QCD_4.

Because YM_2 and gYM_2 are integrable models, so they are useful for exploring the general properties of QCD. For example, one can study the large-N behavior of the free energy of these theories. To do so, one should begin with the partition function of one of these theories on a certain surface. Then the sum over reducible representations of $U(N)$ (or $SU(N)$) appeared in the expressions of the partition function must be replaced by a path integral over continuous Young tableaus and calculated the area-dependence of the free energy from the

Department of Physics, Qom University of Technology, Qom, Iran. email: yalda57L@yahoo.com

saddle-point configuration. In Ref.[29], it was seen that the behavior of the free energy of $U(N)$ YM_2 on a sphere with area $A < A_c = \pi^2$ is logarithmic, and in Ref.[23] for $A > A_c$ the free energy was studied and a third-order phase transition was obtained, at $A = A_c$. A fact that was known earlier in the context of lattice formulation[30]. In Ref.[28], a function G was introduced to charactrize a gYM_2 with the gauge group $U(N)$ on the sphere. In the case of gYM_2 models, the same transition was shown on the sphere for $G(z) = z^4$ in Ref.[28] and for $G(z) = z^6$ and $G(z) = z^2 + \lambda z^4$ in Ref.[31], and also for $G(z) = z^4 + \lambda z^3$ (for small λ) in Ref.[32].

In this paper, the large-N behavior of a gYM_2 based on a gauge group $U(N)$ on a sphere is studied, for which $G(z) = z^4 + \lambda z^n$ $(n < 4)$ and $G(z) = z^6 + \lambda z^n$ $(n < 6)$, and λ is not necessarily small. In "The free energy" section, for $G(z) = z^4 + \lambda z^3$, the free energy seems to experience a zeroth-order phase transition. In "The boundary conditions on density" section, the zeroth-order phase transition is investigated by studying the density ρ and it is obtained that there are four intervals in each of which the density behaves differently. Thus, the free energy on each interval should be investigated separately, and therefore the zeroth-order phase transition is not correct. In "Studying the second subinterval" section, the interval 2) is studied and it is seen that the redefined density on this interval, like initial density, is not nonnegative while it should be nonnegative and therefore the free energy on this interval is undefined and so it must be removed from the corresponding graphs. In "The third-order phase transition" section, the interval 3) is studied and a third-order phase transition at $\tilde{A} = \tilde{A}_{III}$ is obtained. In "The second-order phase transition" section, the interval 3) is studied again and it is seen that there is the other phase transition that is of second order, at $\tilde{A} = \tilde{A}_{IV}$. This is a new result because in all previous papers there were just third-order phase transitions. In "Maxwell construction" section, Maxwell construction is studied. In "Comparing gYM_2 with Maxwell construction" section, gYM_2 and Maxwell construction are compared with each other and it is seen that the main parameters of gYM_2, which are purely mathematical parameters, are similar to the physical parameters in four-dimensional space-time. This result is novel and also so interesting. In "$\phi^6 + \lambda\phi^n (n < 6)$ models" section, a few other models are studied for further research on the outcome of the previous section. This conclusion is so important because it shows a relationship between two-dimensional space-time and four-dimensional space-time and so one can describe an insolvable physical event in four dimensions by studing the appropriate model in two dimensions. "Concluding remarks" section is devoted to the concluding remarks.

The free energy

First, it is helpful to review the expression for the partition function of a gYM_2 on a sphere in the large-N limit[28,32]. The partition function of the gYM_2 on the sphere is[19,20]

$$Z = \sum_r d_r^2 \, e^{-A\Lambda(r)}, \tag{1}$$

where r's are the irreducible representations of the gauge group, d_r is the dimension of the rth representation, A is the area of the sphere and $\Lambda(r)$ is

$$\Lambda(r) = \sum_{k=1}^{p} \frac{a_k}{N^{k-1}} \, C_k(r), \tag{2}$$

in which C_k is the kth Casimir of the group, and a_k's are arbitrary constants. If one considers the gauge group $U(N)$ and parameterizes its representation by N integers $n_1 \geq n_2 \geq ... \geq n_N$, it is seen that[33]

$$\begin{aligned} d_r &= \prod_{1 \leq i \leq j \leq N} \left(1 + \frac{n_i - n_j}{j - i}\right), \\ C_k &= \sum_{i=1}^{N} \left[(n_i + N - i)^k - (N - i)^k\right]. \end{aligned} \tag{3}$$

To make the partition function (1) convergent, it is necessary that p in (2) be even and a_p be positive.

In the large-N limit, the partition function (1) can be rewritten in the form of a path integral over continuous parameters. If the continuous function $\phi(x)$ is introduced as

$$\phi(x) = -n(x) - 1 + x, \tag{4}$$

where

$$0 \leq x := i/N \leq 1, \tag{5}$$

and

$$n(x) := n_i/N, \tag{6}$$

then the partition function (1) becomes

$$Z = \int \prod_{0 \leq x \leq 1} d\phi(x) \, e^{S[\phi(x)]}, \tag{7}$$

where

$$S(\phi) = N^2 \left[-A \int_0^1 dx\, G[\phi(x)] + \int_0^1 \int_0^1 dy\, log|\phi(x) - \phi(y)| \right], \tag{8}$$

apart from an unimportant constant, and

$$G(\phi) = \sum_{k=1}^{p} (-1)^k a_k \phi^k. \tag{9}$$

As $N \to \infty$, for determining the action (8), one should maximize S. The saddle point equation for S is

$$g[\phi(x)] = P \int_0^1 \frac{dy}{\phi(x) - \phi(y)}, \tag{10}$$

where

$$g(\phi) = \frac{A}{2} G'(\phi), \tag{11}$$

and P is the principal value of the integral. If the density is introduced as

$$\rho[\phi(x)] = \frac{dx}{d\phi(x)}, \tag{12}$$

then (10) becomes

$$g(z) = P \int_b^a \frac{\rho(\xi)\, d\xi}{z - \xi}, \tag{13}$$

along with the normalization condition

$$\int_b^a \rho(\xi)\, d\xi = 1. \tag{14}$$

There is also the other condition on the density, that is

$$0 \le \rho(\xi) \le 1. \tag{15}$$

The above condition can be obtained from the condition $n_1 \ge n_2 \ge ... \ge n_N$. To solve (13), the function $H(z)$ is defined in the complex z-plane as[34]

$$H(z) := \int_b^a \frac{\rho(\xi)\, d\xi}{z - \xi}. \tag{16}$$

One can obtain[28]

$$H(z) = g(z) - \sqrt{(z-a)(z-b)} \sum_{m,n,q=0}^{\infty} \frac{(2n-1)!!(2q-1)!!}{2^{n+q} n! q! (n+q+m+1)!} a^n b^q z^m g^{(n+m+q+1)}(0), \tag{17}$$

and

$$\rho(z) = \frac{\sqrt{(a-z)(z-b)}}{\pi} \sum_{m,n,q=0}^{\infty} \frac{(2n-1)!!(2q-1)!!}{2^{n+q} n! q! (n+q+m+1)!} a^n b^q z^m g^{(n+m+q+1)}(0), \tag{18}$$

where $g^{(n)}$ is the nth derivative of g. Using (16) and (14), it is seen that $H(z)$ behaves like z^{-1} for large z. Thus, from (17), one can arrive at

$$\sum_{n,q=0}^{\infty} \frac{(2n-1)!!(2q-1)!!}{2^{n+q} n! q! (n+q)!} a^n b^q g^{(n+q)}(0) = 0, \tag{19}$$

$$\sum_{n,q=0}^{\infty} \frac{(2n-1)!!(2q-1)!!}{2^{n+q} n! q! (n+q-1)!} a^n b^q g^{(n+q-1)}(0) = 1. \tag{20}$$

These two equations should be used to obtain a and b. Defining the free energy as

$$F := -\frac{1}{N^2}\,\ln Z, \tag{21}$$

one can obtain

$$F'(A) = \int_0^1 dx\, G[\phi(x)] = \int_b^a dz\, G(z)\,\rho(z), \tag{22}$$

that $F'(A)$ is the derivative of the free energy with respect to A. Substituting (9) into (22), it is seen that the integrals

$$\int_b^a dz\, z^n\,\rho(z) \tag{23}$$

apear. To obtain these integrals and so $F'(A)$, one should expand $H(z)$ for $z \to \infty$ in (16) and (17).

If one considers

$$G(z) = z^4 + \lambda z^3, \tag{24}$$

by rescaling $\tilde{z} = z/\lambda$, one has

$$G(\tilde{z}) = \lambda^4\left[\tilde{z}^4 + \tilde{z}^3\right]. \tag{25}$$

Using (12), one can obtain

$$\tilde{\rho}(\tilde{z}) = \lambda\rho(z), \tag{26}$$

where

$$\tilde{\rho}(\tilde{z}) := \frac{dx}{d\tilde{z}}. \tag{27}$$

Using (16), one has

$$\tilde{H}(\tilde{z}) = \lambda\, H(z), \tag{28}$$

where

$$\tilde{H}(\tilde{z}) := \int_{\tilde{b}}^{\tilde{a}} d\tilde{\xi}\,\frac{\tilde{\rho}(\tilde{\xi})}{\tilde{z}-\tilde{\xi}}. \tag{29}$$

Using (11) and (17), one obtains

$$\tilde{H}(\tilde{z}) = \tilde{A}\left[\frac{1}{2}(4\tilde{z}^3 + 3\tilde{z}^2) - \frac{1}{4}\sqrt{(\tilde{z}-\tilde{a})(\tilde{z}-\tilde{b})}\,\{3(\tilde{a}+\tilde{b}+2\tilde{z}) + 3(\tilde{a}^2+\tilde{b}^2) + 8\tilde{z}^2 + 2\tilde{a}\tilde{b} + 4\tilde{z}(\tilde{a}+\tilde{b})\}\right], \tag{30}$$

where $\tilde{A} = A\,\lambda^4$. Expanding (30) for large $\tilde{z}$, it is seen that

$$\tilde{H}(\tilde{z}) = \alpha_0 + \alpha_{-1}\tilde{z}^{-1} + O(\tilde{z}^{-2}). \tag{31}$$

Because $\tilde{H}(\tilde{z})$ behaves like $\tilde{z}^{-1}$ for large $\tilde{z}$ as before, so using (30), one arrives at two following equations

$$\tilde{\tau}^2\left(3\tilde{\sigma} + \frac{3}{4}\right) + \tilde{\sigma}^2\left(2\tilde{\sigma} + \frac{3}{2}\right) = 0, \tag{32}$$

$$\frac{3}{4}\tilde{\tau}^4 + \tilde{\tau}^2\left(3\tilde{\sigma}^2 + \frac{3}{2}\tilde{\sigma}\right) = \frac{1}{\tilde{A}}, \tag{33}$$

where

$$\tilde{\sigma} := \frac{\tilde{a}+\tilde{b}}{2}, \tag{34}$$

$$\tilde{\tau} := \frac{\tilde{a}-\tilde{b}}{2}. \tag{35}$$

Using (32) and (33), one obtains

$$\tilde{\tau}^2 = \tilde{\sigma}^2\left(\frac{2\tilde{\sigma}+\frac{3}{2}}{3\tilde{\sigma}+\frac{3}{4}}\right), \tag{36}$$

$$\tilde{A} = -\frac{9\tilde{\sigma}^2+\frac{9}{2}\tilde{\sigma}+\frac{9}{16}}{15\tilde{\sigma}^6+\frac{45}{2}\tilde{\sigma}^5+\frac{171}{16}\tilde{\sigma}^4+\frac{27}{16}\tilde{\sigma}^3}. \tag{37}$$

By applying the condition $\tilde{\tau}^2 \geq 0$ to (36), it is concluded that

$$-\frac{3}{4} \leq \tilde{\sigma} \leq -\frac{1}{4}.$$

Using (36), it is seen that $\tilde{\tau}$ is infinity at $\tilde{\sigma} = -\frac{1}{4}$. Also, using (37), it is seen that $\tilde{A}$ is infinity at $\tilde{\sigma} = -\frac{3}{4}$. Thus, the condition on $\tilde{\sigma}$ is converted to

$$-\frac{3}{4} < \tilde{\sigma} < -\frac{1}{4}. \tag{38}$$

If one expands (16) for large $\tilde{z}$ and uses (14), the derivative of the free energy with respect to the area, using (22) and (24), becomes

$$\tilde{F}'(\tilde{A}) = \tilde{H}_4(\tilde{z}) + \tilde{H}_5(\tilde{z}), \tag{39}$$

where $\tilde{H}_4(\tilde{z})$ (or $\tilde{H}_5(\tilde{z})$) is the coefficient of $\tilde{z}^{-4}$ (or $\tilde{z}^{-5}$) in the expansion of $\tilde{H}(\tilde{z})$. Thus, expanding (30) for large $\tilde{z}$ and using (37), it is seen that

$$\tilde{F}'(\tilde{A}) = -\frac{\tilde{\sigma}^3(36+390\tilde{\sigma}+1667\tilde{\sigma}^2+3500\tilde{\sigma}^3+3600\tilde{\sigma}^4+1600\tilde{\sigma}^5)}{12(1+4\tilde{\sigma})^2(3+15\tilde{\sigma}+20\tilde{\sigma}^2)}. \tag{40}$$

Integrating (40) and using (37), apart from a constant, one can obtain

$$\begin{aligned}\tilde{F}(\tilde{\sigma}) = \frac{1}{4}\Bigg[&-\frac{4}{3+4\tilde{\sigma}} + \frac{3+8\tilde{\sigma}}{2(3+15\tilde{\sigma}+20\tilde{\sigma}^2)^2} + \frac{5(1+4\tilde{\sigma})}{3+15\tilde{\sigma}+20\tilde{\sigma}^2} \\ &-4\log|\tilde{\sigma}| + 2\log|1+4\tilde{\sigma}| - 2\log|3+4\tilde{\sigma}|\Bigg].\end{aligned} \tag{41}$$

Using (41) and (37), one can plot $\tilde{F}$ as a function of $\tilde{A}$ as shown in Fig. 2 and also using (40) and (37), one can plot $\tilde{F}'$ as a function of $\tilde{A}$ as shown in Fig. 3. Since the free energy for a given area must be minimum, so using Fig. 2, it is concluded that the free energy experiences a zeroth-order phase transition. Now the question is whether the zeroth-order phase transition is a correct result or an incorrect one? In the next section, the question will be answered.

The boundary conditions on density

Using (37), one can plot $\tilde{A}$ as a function of $\tilde{\sigma}$ in the interval $\left(-\frac{3}{4}, -\frac{1}{4}\right]$ as shown in Fig. 1. From this figure, it is seen that there are three (or two) values for $\tilde{\sigma}$ for every value of $\tilde{A}$ in the interval $\tilde{A}_I \leq \tilde{A} \leq \tilde{A}_{II}$. Thus, using (41), there are several values for $\tilde{F}$ for any given area in $[\tilde{A}_I, \tilde{A}_{II}]$. For discussing with more detail, first one should study the density and then return to calculate the free energy. Thus, one can begin with (11) and (18) and find the density for $\tilde{G}(\tilde{z}) = \tilde{z}^4 + \tilde{z}^3$. The density becomes

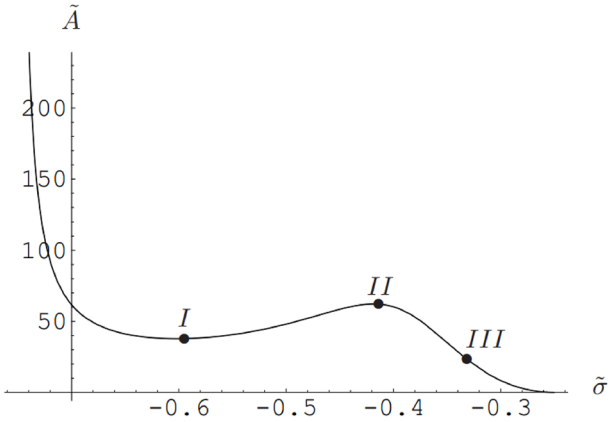

Figure 1. Surface area.

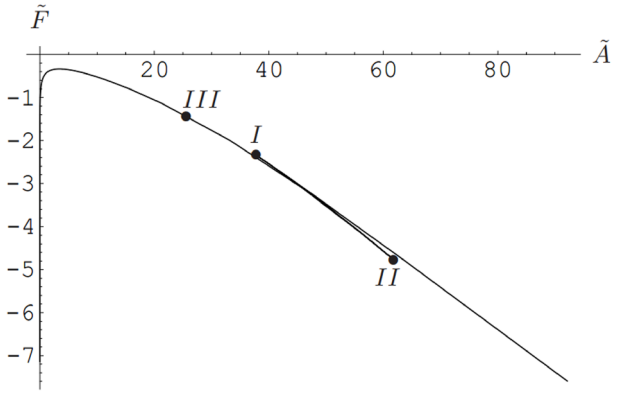

Figure 2. Free energy.

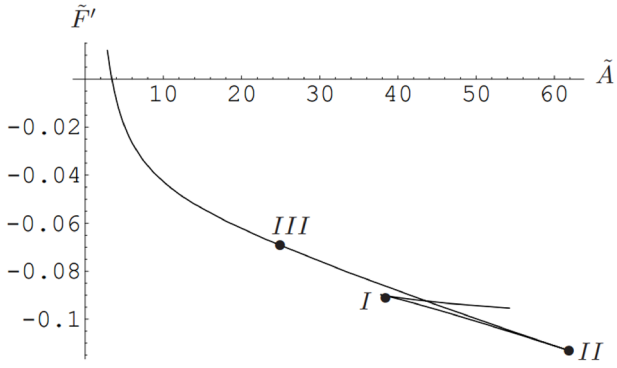

Figure 3. The derivative of the free energy.

$$\tilde{\rho}(\tilde{z}) = \frac{\tilde{A}}{2\pi}\sqrt{\tilde{\tau}^2 - (\tilde{z}-\tilde{\sigma})^2}\left[4\tilde{\sigma}^2 + 2\tilde{\tau}^2 + 4\tilde{\sigma}\tilde{z} + 4\tilde{z}^2 + 3(\tilde{\sigma}+\tilde{z})\right]. \tag{42}$$

By differentiating $\tilde{\rho}$ with respect to $\tilde{z}$ and putting the derivative equal to zero, one obtains

$$6(1+4\tilde{\sigma})\,\tilde{z}^3 + \{3+6\tilde{\sigma}(1-4\tilde{\sigma})\}\,\tilde{z}^2 + \tilde{\sigma}(-3-6\tilde{\sigma}+8\tilde{\sigma}^2)\,\tilde{z} + \tilde{\sigma}^2(1+2\tilde{\sigma})(3+4\tilde{\sigma}) = 0. \tag{43}$$

This equation has three roots $\tilde{z}_i$'s for which the density is extremum. One can plot $\tilde{z}_i$'s and also $\tilde{b}$ and $\tilde{a}$ (using (34), (35) and (36)) as functions of $\tilde{\sigma}$ on the interval $-\frac{3}{4} < \tilde{\sigma} < -\frac{1}{4}$ as shown in Fig. 4. Because the density has been defined only on the interval $\tilde{b} \le \tilde{z} \le \tilde{a}$, so using Fig. 4, it is seen that there are three subintervals ($\tilde{\sigma} \le \tilde{\sigma}_I, \tilde{\sigma}_I \le \tilde{\sigma} \le \tilde{\sigma}_{II}, \tilde{\sigma} \ge \tilde{\sigma}_{II}$) on each of which the number of $\tilde{z}_i$'s is different and so the density on each

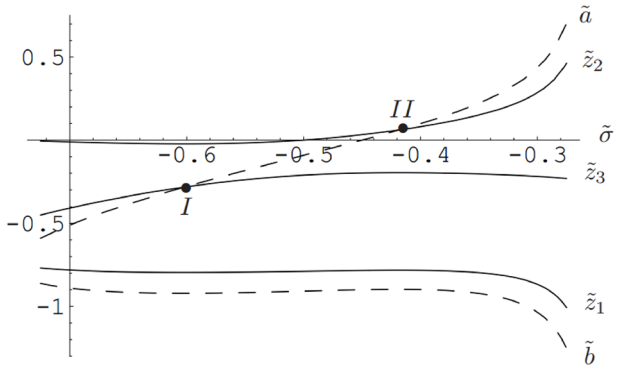

Figure 4. The roots of the density.

subinterval should be plotted separately. The graphs of these densities have been shown in Figs. 5, 6 and 7. Each of these figures is related to a specific $\tilde{\sigma}$. Changing the value of $\tilde{\sigma}$, the curves in Figs. 5 and 6 change quantitatively but don't change qualitatively. For some $\tilde{\sigma}$'s, Fig. 7 is converted to Fig. 8. To find the boundary of Figs. 7 and 8, one should obtain the $\tilde{\sigma}$ for which the minimum value of $\tilde{\rho}$ with respect to $\tilde{z}$ becomes zero. Thus one should plot $\tilde{\rho}_i$'s, which are the extrema of $\tilde{\rho}(\tilde{z})$, as functions of $\tilde{\sigma}$ (Fig. 9). Using Figs. 4 and 9, it is seen that there are four subintervals for $\tilde{\sigma}$ as follows: 1) $-\frac{3}{4} < \tilde{\sigma} \leq \tilde{\sigma}_I$, 2) $\tilde{\sigma}_I \leq \tilde{\sigma} \leq \tilde{\sigma}_{II}$, 3) $\tilde{\sigma}_{II} \leq \tilde{\sigma} \leq \tilde{\sigma}_{III}$, and 4) $\tilde{\sigma}_{III} \leq \tilde{\sigma} < -\frac{1}{4}$ that the densities of these subintervals have been shown in Figs. 5, 6, 7 and 8, respectively. The condition (using 26 and 15)

$$0 \leq \tilde{\rho} \leq \lambda \tag{44}$$

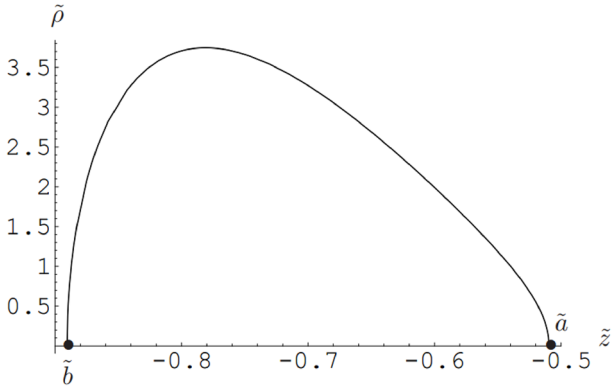

Figure 5. The density in subinterval 1).

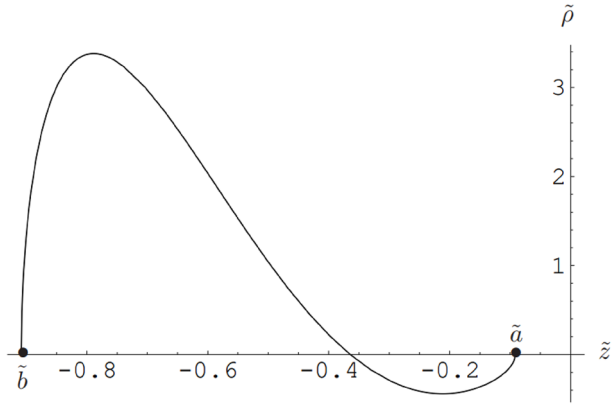

Figure 6. The density in subinterval 2).

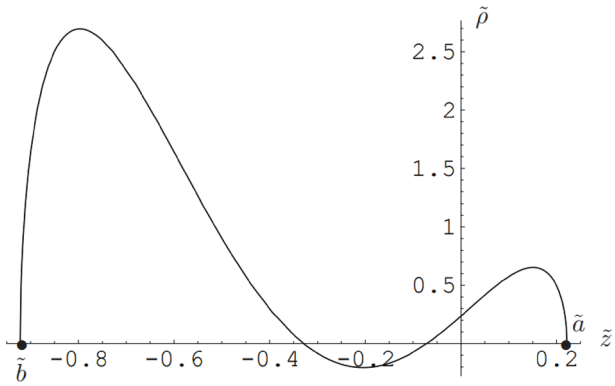

Figure 7. The density in subinterval 3).

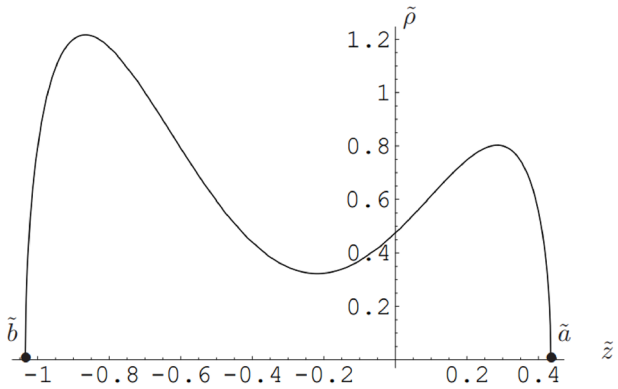

Figure 8. The density in subinterval 4).

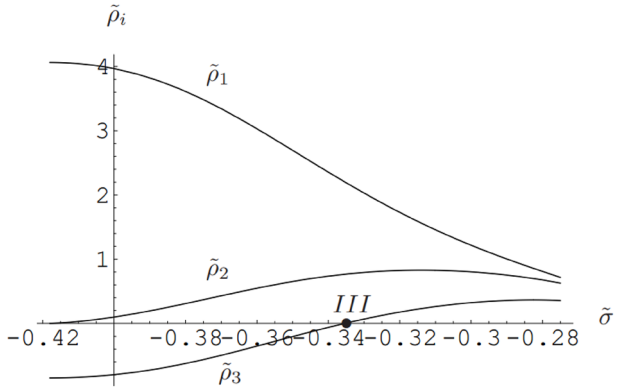

Figure 9. The extremum densities.

restricts the acceptable densities. Because $\tilde{\rho}$ is not nonnegative on the subintervals 2) and 3), first one should redefine the density on these subintervals and then find the free energies of these redefined densities. Thus, the free energy of the system is changed. As a result, the zeroth-order phase transition obtained in the previous section is incorrect. In the next three sections, the density on two subintervals 2) and 3) will be redefined and the order of the phase transition will be obtained.

Studying the second subinterval

One can obtain $\tilde{\sigma}_I = -0.601986$ and $\tilde{\sigma}_{II} = -0.418476$, and also $\tilde{A}_I = 37.8042$ and $\tilde{A}_{II} = 62.2248$. From Fig. 6, it is seen that the density is not nonnegative on this subinterval so it must be redefined. If one redefines it as

$$\tilde{\rho}_2(\tilde{z}) = \begin{cases} 0, & \tilde{z} \in [\tilde{c}, \tilde{a}] \\ \overline{\rho}_2(\tilde{z}), & \tilde{z} \in [\tilde{b}, \tilde{c}] \end{cases} \tag{45}$$

and finds $\overline{\rho}_2(\tilde{z})$ as a function of $\tilde{\delta}$ where $\tilde{\delta} = \frac{\tilde{b}+\tilde{c}}{2}$, it is seen that $\overline{\rho}_2(\tilde{z})$ (as a function of $\tilde{\delta}$) is the same as $\tilde{\rho}_2(\tilde{z})$ (as a function of $\tilde{\sigma}$). Thus, the behavior of $\overline{\rho}_2(\tilde{z})$ is similar to that of $\tilde{\rho}_2(\tilde{z})$ but on the interval $\tilde{b} \le \tilde{z} \le \tilde{c}$. This means that $\overline{\rho}_2(\tilde{z})$ is negative for some $\tilde{z}$'s. Thus, this redefining of the density is incorrect. If it is redefined as

$$\tilde{\rho}_2(\tilde{z}) = \begin{cases} 0, & \tilde{z} \in [\tilde{d}, \tilde{e}] \\ \overline{\rho}_2(\tilde{z}), & \tilde{z} \in [\tilde{b}, \tilde{d}] \cup [\tilde{e}, \tilde{a}] \end{cases} \tag{46}$$

one can find[28]

$$\tilde{H}_2(\tilde{z}) = \frac{\tilde{A}}{2}\left[(4\tilde{z}^3 + 3\tilde{z}^2) - \sqrt{(\tilde{z}-\tilde{b})(\tilde{z}-\tilde{d})(\tilde{z}-\tilde{e})(\tilde{z}-\tilde{a})}\,\{3 + 4\tilde{z} + 2(\tilde{a}+\tilde{b}+\tilde{d}+\tilde{e})\}\right], \tag{47}$$

and

$$\tilde{\rho}_2(\tilde{z}) = \frac{\tilde{A}}{2\pi}\sqrt{(\tilde{z}-\tilde{b})(\tilde{z}-\tilde{d})(\tilde{z}-\tilde{e})(\tilde{a}-\tilde{z})}\,\{3 + 4\tilde{z} + 2(\tilde{a}+\tilde{b}+\tilde{d}+\tilde{e})\}. \tag{48}$$

Expanding $\tilde{H}(\tilde{z})$ for large $\tilde{z}$, it is seen that

$$\tilde{H}_2(\tilde{z}) = \beta_1\tilde{z} + \beta_0 + \beta_{-1}\tilde{z}^{-1} + O(\tilde{z}^{-2}). \tag{49}$$

Because $\tilde{H}_2(\tilde{z})$ should behave like $\tilde{z}^{-1}$ for large $\tilde{z}$, so one arrives at the following three equations

$$\beta_1 = 0, \tag{50}$$

$$\beta_0 = 0, \tag{51}$$

$$\beta_{-1} = 1. \tag{52}$$

One also has[28]

$$\int_{\tilde{d}}^{\tilde{e}} d\tilde{z}\{g(\tilde{z}) - \tilde{H}_2(\tilde{z})\} = 0, \tag{53}$$

where $g(\tilde{z}) = \frac{\tilde{A}}{2} G'(\tilde{z})$. Thus, one can obtain

$$\int_{\tilde{d}}^{\tilde{e}} d\tilde{z}\left[\frac{\tilde{A}}{2}\sqrt{(\tilde{z}-\tilde{b})(\tilde{z}-\tilde{d})(\tilde{z}-\tilde{e})(\tilde{z}-\tilde{a})}\,\{3+4\tilde{z}+2(\tilde{a}+\tilde{b}+\tilde{d}+\tilde{e})\}\right] = 0. \tag{54}$$

Using this equation and (50), (51) and (52), one can obtain the four unknowns $\tilde{a}, \tilde{b}, \tilde{e}$ and $\tilde{d}$. To study the structure of the phase transition, one can use the following change of variables

$$\tilde{b} = \tilde{b}_c(1+P), \quad \tilde{d} = \tilde{d}_c(1+M), \quad \tilde{e} = \tilde{e}_c(1+X), \quad \tilde{a} = \tilde{a}_c(1+U), \tag{55}$$

where the index c shows a critical point between subintervals 1) and 2), that is labeled *I* in Figs. 1, 2, 3, 4, 5, 6, 7, 8, 9, 10, 11 and 12. By calculating, it is seen that

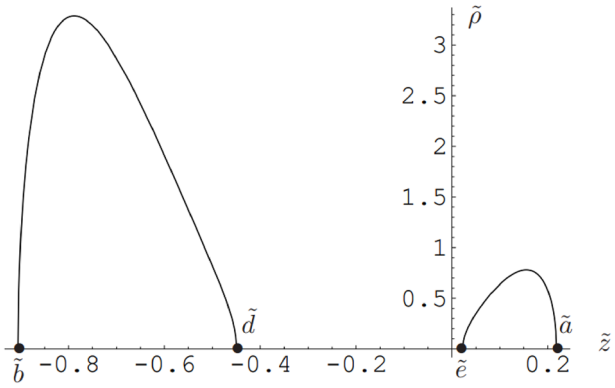

Figure 10. The redefined density.

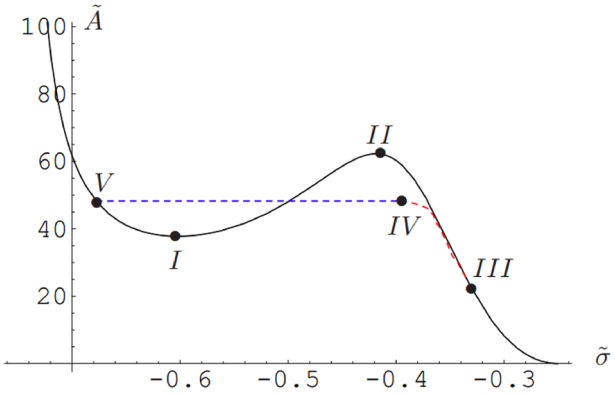

Figure 11. The modified surface area.

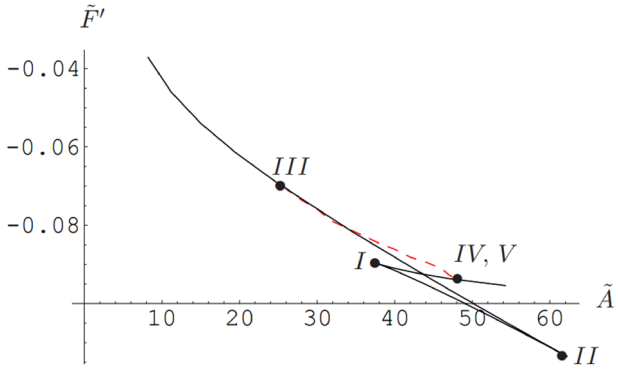

Figure 12. The modified derivtive of the free energy.

$$\tilde{b}_c = -0.920721, \quad \tilde{d}_c = \tilde{e}_c = \tilde{a}_c = -0.283251 \tag{56}$$

One can substitute (55) and (56) into (50) and (51), and obtain

$$\begin{aligned} P = &-0.12M - 0.06M^2 - 0.12U - 0.06U^2 - 0.12X \\ &-0.06X^2 - 0.04MU - 0.04UX - 0.04MX, \end{aligned} \tag{57}$$

$$U = -M - 0.232M^2 - X - 0.232X^2 - 0.232MX. \tag{58}$$

Using these two relations, it can be seen that if $M = -X$ then P, U, X^2 and M^2 are of the same order, but if $M \neq -X$ then P, M, X and U are of the same order. If $M = -X$, using (55) and (56), it is seen that $\tilde{a} < \tilde{e}$. This is an incorrect result because there is the following condition on $\tilde{b}$, $\tilde{d}$, $\tilde{e}$ and $\tilde{a}$ (using (46))

$$\tilde{b} < \tilde{d} < \tilde{e} < \tilde{a}, \tag{59}$$

so $M \neq -X$. One can consider

$$\begin{aligned} P =& P_{1/2}\,\Omega^{1/2} + P_1\,\Omega + P_{3/2}\,\Omega^{3/2} + P_2\,\Omega^2, \\ M =& M_{1/2}\,\Omega^{1/2} + M_1\,\Omega + M_{3/2}\,\Omega^{3/2} + M_2\,\Omega^2, \\ X =& X_{1/2}\,\Omega^{1/2} + X_1\,\Omega + X_{3/2}\,\Omega^{3/2} + X_2\,\Omega^2, \\ U =& U_{1/2}\,\Omega^{1/2} + U_1\,\Omega + U_{3/2}\,\Omega^{3/2} + U_2\,\Omega^2, \end{aligned} \tag{60}$$

where Ω is $(\tilde{A} - \tilde{A}_c)/\tilde{A}_c$ and $\tilde{A}_c = \tilde{A}_I$. From (55), (56), (60), and also (50), (51), (52) and (54), one can obtain

$$\begin{aligned} P =& -0.067\,\Omega + 0.0127\,\Omega^{3/2} + 0.05\,\Omega^2, \\ M =& 0.64\,\Omega^{1/2} - 0.064\,\Omega - 0.266\,\Omega^{3/2} + X_2\,\Omega^2, \\ X =& 0.64\,\Omega^{1/2} - 0.064\,\Omega - 0.266\,\Omega^{3/2} + X_2\,\Omega^2, \\ U =& -1.28\,\Omega^{1/2} - 0.16\,\Omega + 0.34\,\Omega^{3/2} + (0.038 - 2X_2)\,\Omega^2. \end{aligned} \tag{61}$$

Using (61), (55), (56), (48) and $\tilde{A} = \tilde{A}_I\,(1 + \Omega)$, one can plot the density as a function of $\tilde{z}$ for small Ω. It is seen that for $\Omega \neq 0$, this graph is similar to Fig. 6. Thus, the redefined density is not also nonnegative. It follows that the subinterval 2) must not exist and the curves between *I* and *II* shown in Figs. 1, 2 and 3 must be removed.

The third-order phase transition

The subinterval 3) is $\tilde{\sigma}_{II} \leq \tilde{\sigma} \leq \tilde{\sigma}_{III}$. One can obtain $\tilde{\sigma}_{II} = -0.418476$ and $\tilde{\sigma}_{III} = -0.33541$, and also $\tilde{A}_{II} = 62.2248$ and $\tilde{A}_{III} = 25.5689$. From Fig. 7, it is seen that the density is not nonnegative on this subinterval, so it must be redefined and the curves between *II* and *III* shown in Figs. 1, 2 and 3 must be replaced by new curves obtained in the next section. In line with the previous section, if one redefines the density as

$$\tilde{\rho}_3(\tilde{z}) = \begin{cases} 0, & \tilde{z} \in [\tilde{d}, \tilde{e}] \\ \overline{\rho}_3(\tilde{z}), & \tilde{z} \in [\tilde{b}, \tilde{d}] \cup [\tilde{e}, \tilde{a}] \end{cases} \tag{62}$$

it can be concluded that Eqs. (47) to (54), which were obtained by studying the second subinterval, are also valid for the subinterval 3). To study the structure of the phase transition at the point *III*, one can use the following change of variables

$$\tilde{b} = \tilde{b}_{III}(1 + P), \quad \tilde{d} = \tilde{d}_{III}(1 + M), \quad \tilde{e} = \tilde{e}_{III}(1 + X), \quad \tilde{a} = \tilde{a}_{III}(1 + U), \tag{63}$$

where

$$\tilde{b}_{III} = -0.938782, \quad \tilde{a}_{III} = 0.267962, \quad \tilde{d}_{III} = \tilde{e}_{III} = -0.207295. \tag{64}$$

Substituting (63) and (64) into (50) and (51), one can obtain

$$\begin{aligned} P &= -0.047\, M^2 - 018\, U - 0.03\, MX - 0.047\, X^2, \\ U &= -0.15\, M^2 - 0.1\, MX - 0.15\, X^2. \end{aligned} \tag{65}$$

Using these two relations, it is seen that P, U, M^2 and X^2 are of the same order. Thus, one can consider

$$\begin{aligned} P =& P_1\, \Omega + P_{3/2}\, \Omega^{3/2} + P_2\, \Omega^2, \\ M =& M_{1/2}\, \Omega^{1/2} + M_1\, \Omega + M_{3/2}\, \Omega^{3/2} + M_2\, \Omega^2, \\ X =& X_{1/2}\, \Omega^{1/2} + X_1\, \Omega + X_{3/2}\, \Omega^{3/2} + X_2\, \Omega^2, \\ U =& U_1\, \Omega + U_{3/2}\, \Omega^{3/2} + U_2\, \Omega^2, \end{aligned} \tag{66}$$

where $\Omega = \frac{\tilde{A} - \tilde{A}_{III}}{\tilde{A}_{III}}$. Substituting (63), (64) and (66) into (50), (51), (52) and (54), it is obtained

$$\begin{aligned} P =& -0.064\, \Omega + 0.048\, \Omega^2, \\ M =& 1.61\, \Omega^{1/2} - 0.125\, \Omega - 0.498\, \Omega^{3/2} + (-0.01 - X_2)\, \Omega^2, \\ X =& -1.61\, \Omega^{1/2} - 0.125\, \Omega + 0.498\, \Omega^{3/2} + X_2\, \Omega^2, \\ U =& -0.535\, \Omega + 0.18\, \Omega^2. \end{aligned} \tag{67}$$

Using (63), (64), (67), (48) and $\tilde{A} = \tilde{A}_{III}\,(1 + \Omega)$, one can plot the density as a function of $\tilde{z}$ for small Ω as shown in Fig. 10. It is seen that the density is nonnegative for $\Omega \neq 0$, so the redefinition of the density as (62) on the subinterval 3) near the point *III* is correct. Now one can obtain the phase transition near the point *III*. Expanding (47) for large $\tilde{z}$ and using (39), one can obtain

$$(\tilde{F}_3')_{III}(\tilde{A}) = -0.07 - 0.034\, \Omega + 0.0129\, \Omega^2 + O(\Omega^3). \tag{68}$$

To calculate the phase transition, one should find $\tilde{F}_w'(\tilde{A})$ near the point *III*, which is the derivative of the free energy obtained using the initial density (42). Substituting $\tilde{\sigma} = \Phi + \tilde{\sigma}_{III}$ into (37) and using $\tilde{A} = \tilde{A}_{III}\,(1 + \Omega)$, one gets

$$\Phi = -0.0414\, \Omega + 0.00747\, \Omega^2. \tag{69}$$

Thus, using (40), it is obtained

$$(\tilde{F}_w')_{III}(\tilde{A}) = -0.07 - 0.034\, \Omega + 0.0066\, \Omega^2 + O(\Omega^3). \tag{70}$$

Using (68) and (70), it is concluded

$$(\tilde{F}_3')_{III}(\tilde{A}) - (\tilde{F}_w')_{III}(\tilde{A}) = 0.0063\, \Omega^2 + O(\Omega^3). \tag{71}$$

As a result, there is a third-order phase transition near the point *III* on the subinterval 3).

The second-order phase transition

As seen in the previous section, in Fig. 1, if one moves on the graph from the right side to the left passing through the point *III*, Fig. 8 is converted to Fig. 7. Thus, the density must be redefined as (62) on the interval 3) and as a result Fig. 7 will be replaced by Fig. 10. In this section, it is seen that by increasing $\tilde{A}$ continuously from $\tilde{A}_{III}$ to $\tilde{A}_{IV}$ in Fig. 11, the distance between $\tilde{e}$ and $\tilde{a}$ goes to zero in Fig. 10. Thus, the curve between the points *III* and *II* in Fig. 1 will be replaced by the curve between the points *III* and *IV* in Fig. 11. Also, as seen in "Studying the second subinterval" section, the curve between the points *I* and *II* must be removed. Thus, the graph of the area versus $\tilde{\sigma}$ is converted to the curve from the left side to the point *I* and the curve from the point *IV* to the right side in Fig. 11. It was seen that the graph of the density as a function of $\tilde{z}$ was similar to Fig. 5 for $\tilde{\sigma}_V < \tilde{\sigma} < \tilde{\sigma}_I$, while it is seen that the graph is similar to Fig. 10 for $\tilde{\sigma}_{IV} < \tilde{\sigma} < \tilde{\sigma}_{III}$. Using the fact that there is a specific density for a given area and the graph of the density by increasing $\tilde{A}$ should be continuously converted from Figs. 8, 9 and 10 and finally to Fig. 5, the curve between *I* and *V* must be removed too. Thus, in Figs. 11 and 12, the solid curves from *V* to *III* are replaced by the dashed curves.

In this section, first, the points *IV* and *V* will be found and then the phase transition, to go from *IV* to *V*, will be obtained.

At the point *IV*, $\tilde{a}$ and $\tilde{e}$ are equal because the density at the point *IV* is the same as one at the point *V* and so the graph of the density at the point *IV* is like Fig. 5. Thus, one can use the following change of variables

$$\tilde{a} = \tilde{e} = \nu, \quad \tilde{d} = \gamma + \eta, \quad \tilde{b} = \gamma - \eta. \tag{72}$$

Using (50), one obtains

$$\eta^2 = -\frac{4\gamma^2 + (\gamma+\nu)(3+4\nu)}{2}. \tag{73}$$

Now, using (51), (52) and the above relations, the following two equations are obtained

$$-2\gamma\nu(3+4\gamma+4\nu) - \frac{1}{2}(3+8\gamma)\{4\gamma^2 + (\gamma+\nu)(3+4\nu)\} = 0, \tag{74}$$

$$-\frac{3}{16}\{\gamma + 4\gamma^2 - 4\gamma\nu - \nu(3+4\nu)\}\{4\gamma^2 + (\gamma+\nu)(3+4\nu)\}\tilde{A} = 1. \tag{75}$$

The roots of Eq. (74) are

$$\nu_1 = -\frac{9 + 48(\gamma+\gamma^2) + \sqrt{81 + 432\gamma - 288\gamma^2 - 3840\gamma^3 - 3840\gamma^4}}{24 + 96\gamma} \tag{76}$$

and

$$\nu_2 = -\frac{9 + 48(\gamma+\gamma^2) - \sqrt{81 + 432\gamma - 288\gamma^2 - 3840\gamma^3 - 3840\gamma^4}}{24 + 96\gamma}. \tag{77}$$

Substituting (72) and (73) into (54), one has

$$\int_{\gamma+\eta}^{\nu} d\tilde{z}\left[\frac{\tilde{A}}{2}(3+4\tilde{z}+4\gamma+4\nu)(\tilde{z}-\nu)\sqrt{\tilde{z}^2 - 2\tilde{z}\gamma + \frac{1}{2}\{6\gamma^2 + (\gamma+\nu)(3+4\nu)\}}\right] = 0. \tag{78}$$

Now, one should calculate this integral and substitute (76) and (77) for ν in the result of the integral, one by one. Using ν_1, one can obtain

$$(\gamma_1 = -0.67748,\ \tilde{A}_1 = 48.2053), \quad (\gamma_2 = -0.42,\ \tilde{A}_2 = 62.2), \tag{79}$$

and using ν_2, one can get

$$\gamma_3 = -0.602, \quad \tilde{A}_3 = 37.8042, \tag{80}$$

that (75) has been used to obtain $\tilde{A}_i$'s. At this step, one should study $\tilde{A}_1$, $\tilde{A}_2$ and $\tilde{A}_3$ to find the point *IV*. It is seen that the graph of the density for $\tilde{A} = \tilde{A}_2$ is like Fig. 6 that is not nonnegative, so this answer is incorrect. On the other hand, the graphs of the density for both $\tilde{A}_1$ and $\tilde{A}_3$ are like Fig. 5. Thus, to investigate which answer is correct, one should find the point *IV* numerically. Using (50), (51), (52) and (54) and starting from the point *III*, by increasing $\tilde{A}$ little by little and using the relations in the subinterval 3), one can obtain $\tilde{b} = -0.9069$, $\tilde{d} = -0.4689$, $\tilde{e} = -0.09765$ and $\tilde{a} = 0.2117$ for $\tilde{A} = \tilde{A}_3$. Thus, this answer is unacceptable because the initial condition $\tilde{e} = \tilde{a}$ is not satisfied for $\tilde{A} = \tilde{A}_3$. Increasing $\tilde{A}$ further, for $\tilde{A} = \tilde{A}_1$, one can plot the density as a function of $\tilde{z}$. It is seen that the graph is like Fig. 5, and so the point *IV* is specified by $\tilde{A}_1$, γ_1, and ν_1. Thus, the numerical values of the unknown parameters at the point *IV* are as follows

$$\tilde{A}_{IV} = 48.2053, \quad \tilde{a}_{IV} = \tilde{e}_{IV} = 0.12023, \quad \tilde{d}_{IV} = -0.44966, \quad \tilde{b}_{IV} = -0.905313 \tag{81}$$

Using

$$\tilde{b} = \tilde{b}_{IV}(1+P), \quad \tilde{d} = \tilde{d}_{IV}(1+M), \quad \tilde{e} = \tilde{e}_{IV}(1+X), \quad \tilde{a} = \tilde{a}_{IV}(1+U) \tag{82}$$

and also using (50) and (51), one can obtain

$$\begin{aligned} P &= 0.0729\,U + 0.0729\,X + 0.03699\,U^2 + 0.03699\,X^2 + 0.0306\,UX, \\ M &= -5.584P - 0.3257U - 0.3257X - 0.0938U^2 - 0.0938X^2 - 0.0626UX. \end{aligned} \tag{83}$$

Using these two relations, it is clear that if $U = -X$ then P, M, U^2 and X^2 are of the same order, but if $U \neq -X$ then P, M, U and X are of the same order.

Thus, for $U \neq -X$, one can consider

$$\begin{aligned} P &= P_1\,\Omega + P_2\,\Omega^2 \\ M &= M_1\,\Omega + M_2\,\Omega^2 \\ U &= U_1\,\Omega + U_2\,\Omega^2 \\ X &= X_1\,\Omega + X_2\,\Omega^2, \end{aligned} \tag{84}$$

where $\Omega = \frac{\tilde{A}-\tilde{A}_{IV}}{\tilde{A}_{IV}}$ and so Ω is negative on the subinterval 3). One can use (50), (51), (52) and (54) to calculate the unknown parameters P_1 to X_2 that two sets of vaues are obtained. Using one of these sets, it is seen that $X = -0.9375\,\Omega$, and $U = -.0057\,\Omega$. Using (81) and (82), the inequality $\tilde{a} < \tilde{e}$ is obtained that is incorrect

because $\tilde{b} < \tilde{d} < \tilde{e} < \tilde{a}$. Using the other one, it is seen that $\tilde{e} = \tilde{a}$, up to $O(\Omega^2)$, so this is incorrect too. Thus, $U \neq -X$ is not acceptable, and so $U = -X$.

For $U = -X$, one can expand (50) and (51) up to order P and obtain

$$P = 0.04\,X^2, \quad M = -0.36\,X^2. \tag{85}$$

Using (85), (52) and $\tilde{A} = \tilde{A}_{IV}\,(1 + \Omega)$, it is obtained (up to order $\sqrt{\Omega}$)

$$(X)_1 = -1.15\,i\sqrt{\Omega}, \quad (X)_2 = 1.15\,i\sqrt{\Omega}. \tag{86}$$

Because Ω is negative and $U = -X$, so the correct answer (up to order $\sqrt{\Omega}$) is $X = 1.15\,i\sqrt{\Omega}$. Thus, one can obtain

$$X = 1.15\,i\sqrt{\Omega} + X_1\,\Omega, \quad U = -1.15\,i\sqrt{\Omega} - X_1\,\Omega, \quad P = -0.057\Omega, \quad M = 0.487\Omega. \tag{87}$$

Expanding $\tilde{H}(\tilde{z})$ for large $\tilde{z}$ and using $\tilde{F}_3'(\tilde{A}) = \tilde{H}_4(\tilde{z}) + \tilde{H}_5(\tilde{z})$ near the point IV, it is seen that

$$(\tilde{F}_3')_{IV}\,(\tilde{A}) = -0.09396 - 0.031046\,\Omega + O(\Omega^2). \tag{88}$$

Now, one should find the point V that is in the subinterval 1) and $\tilde{A}_V = \tilde{A}_{IV} = 48.2053$. Because the areas related to the points V and IV are the same , so the graphs of the density at these two points must be the same qualitativey and also quantitatively. It can be concluded that

$$\tilde{a}_V = \tilde{d}_{IV} = -0.44966, \quad \tilde{b}_V = \tilde{b}_{IV} = -0.905313, \quad \tilde{\sigma}_V = -0.6775 \tag{89}$$

Thus, one can obtain $\tilde{F}_w'$ near the point V, like "The third-order phase transition" section. Up to order Ω, one can arrive at

$$(\tilde{F}_w')_V\,(\tilde{A}) = -0.09396 - 0.013411\,\Omega + O(\Omega^2). \tag{90}$$

Using (88) and (90), it is seen that

$$(\tilde{F}_3')_{IV}\,(\tilde{A}) - (\tilde{F}_w')_V\,(\tilde{A}) = -0.017635\,\Omega + O(\Omega^2). \tag{91}$$

It is clear that there is a second-order phase transition and $(\tilde{F}_3')_{IV}\,(\tilde{A}) > (\tilde{F}_w')_V\,(\tilde{A})$ because Ω is negative.This is a new result because in all previous papers there were just third-order phase transitions. Now, one can plot $\tilde{F}'$ as a function of $\tilde{A}$ as shown in Fig. 12. In this figure, the solid curves from I to II, I to V, and II to III must be replaced by the dashed curve from III to IV. Meanwhile, in Fig. 12 there are two regions resembling triangles, and the surface areas of these two triangles should be the same. The proof for that comes from the fact that one can go from the point III to the point IV through two different paths, the wrong one which goes through the lower curve (III to II, II to I, and then I to IV), and the correct one which goes from III to IV directly. The difference of the free energies at IV and III should be the same following both paths. This results that the surface areas of the triangle-like regions are equal.

Maxwell construction

Van der Waals equation of state for a gas is

$$\left(p + \frac{an^2}{V^2}\right)(V - nb) = nRT, \tag{92}$$

where n is the number of moles, T is temperature, p is pressure, and V is the total volume of the gas. R is the gas constant that is $R = 8.3145\ \frac{\mathrm{J}}{\mathrm{mol.K}}$. a and b are positive experimental constants that are specific for any specified gas. This relation, can also be rewritten as

$$\left(p + \frac{a'}{v^2}\right)(v - b') = k_B T, \tag{93}$$

where $b' = \frac{b}{N_A}$, $a' = \frac{a}{N_A^2}$, $v = \frac{V}{N}$ (N is the total number of particles), $k_B = 1.38 \times 10^{-23}\ \frac{\mathrm{J}}{\mathrm{K}}$ that is Boltzmann's constant, and $N_A = 6.02 \times 10^{23}$ that is Avogadro's number. Using above relation, it is seen that in the inflection point, using

$$\frac{\partial p}{\partial v}|_c = 0, \quad \frac{\partial^2 p}{\partial v^2}|_c = 0, \tag{94}$$

there are the following three conditions

$$v_c = 3b', \quad T_c = \frac{8a'}{27b'k_B}, \quad p_c = \frac{a'}{27b'^2}. \tag{95}$$

The point with these conditions is named critical point. If (93) is rewritten in terms of $\tilde{v}$, $\tilde{p}$ and $\tilde{T}$ where

$$\tilde{v} = \frac{v}{v_c}, \quad \tilde{p} = \frac{p}{p_c}, \quad \tilde{T} = \frac{T}{T_c}, \tag{96}$$

then (93) is converted to

$$(3\tilde{v} - 1)\left(\tilde{p} + \frac{3}{\tilde{v}^2}\right) = 8\tilde{T}. \tag{97}$$

It is seen that the above relation is independent of a' and b'. Now, one can plot $\tilde{p}$ as a function of $\tilde{v}$ (for van der Waals isotherms) for $T = T_c$, $T > T_c$, and $T < T_c$ as shown in Fig. 13. In Fig. 14 that is for $T < T_c$, the solid curve between 1 and 2 should be removed and 1 must be connected to 2 directly and, meanwhile, the surface areas of regions B and C should be the same[35]. If one plots chemical potential as a function of pressure, as shown in Fig. 15, comparing with Fig. 14, the region resembling triangle should be removed from the graph. Thus, the chemical potential experiences a first-order phase transition at the point 1 (or 2) and as a result the free energy of the substance experiences a second-order phase transition because the chemical potential is derivative of the free energy.

Comparing *gYM*$_2$ with Maxwell construction

Comparing Figs. 11 and 14 and also Figs. 12 and 15, it is seen that $\tilde{A}$ is equivalent to pressure, $\tilde{\sigma}$ is equivalent to volume and $\tilde{F}'$ is equivalent to chemical potential. The points V and IV in gYM_2 are equivalent to the points 1 and 2 in Maxwell construction, respectively. The free energy of the system experiences a second-order phase transition to go from V to IV, and also the same transition occurs to go from 1 to 2. The surface areas of regions B and C in Fig. 14 are the same and also the surface areas of the triangle-like regions in Fig. 12 are the same.

If one considers $G(z) = z^4 + \lambda z^2$ instead of $G(z) = z^4 + \lambda z^3$, and uses the relations of "The free energy" section, it is seen that $\tilde{\tau}^2$ is negative for all $\tilde{\sigma}$. Thus, there is no real answer.

However, if one considers $G(z) = z^4 + \lambda z$ instead of $G(z) = z^4 + \lambda z^3$, and uses "The free energy" section, it is obtained

$$\tilde{A} = \frac{48\tilde{\sigma}^2}{1 - 16\tilde{\sigma}^3 - 80\tilde{\sigma}^6}, \tag{98}$$

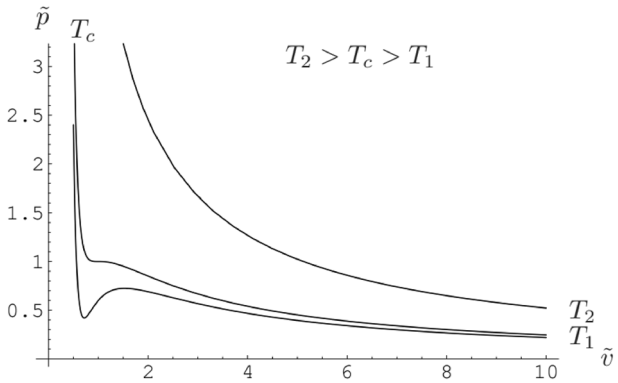

Figure 13. Pressure as a function of volume(isotherms).

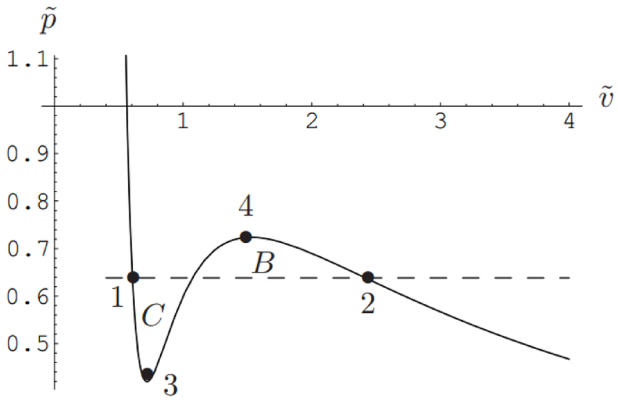

Figure 14. Pressure as a function of volume for $T < T_c$.

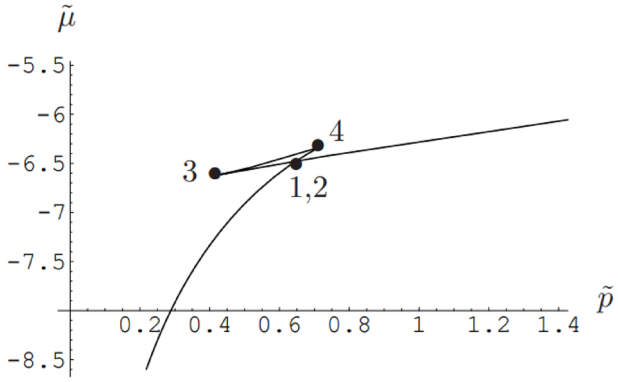

Figure 15. Chemical potential as a function of pressure for $T < T_c$.

where $\tilde{A} = A\,\lambda^{4/3}$ and $\tilde{\sigma} = \frac{\sigma}{\lambda^{1/3}}$. Thus, one can plot $\tilde{A}$ as a function of $\tilde{\sigma}$ as shown in Fig. 16. This figure is similar to Fig. 13 for $T > T_c$.

As a result, $G(z)$ in gYM_2 plays the role of temperature in Maxwell construction. This comparison is completety new and there is not like this in other papers.

$\phi^6 + \lambda\phi^n (n < 6)$ models

To complete the previous section, one should study more models such as $\phi^6 + \lambda\,\phi^n (n < 6)$. If

$$G(z) = z^6 + \lambda z^5, \tag{99}$$

by rescaling $\tilde{z} = z/\lambda$, and using (11) and (17), one can obtain

$$\begin{aligned}\tilde{H}(\tilde{z}) =& \tilde{A}\left[\frac{1}{2}(6\tilde{z}^5 + 5\tilde{z}^4) - \frac{1}{128}\sqrt{(\tilde{z}-\tilde{a})(\tilde{z}-\tilde{b})}\,\{105(\tilde{a}^4 + \tilde{b}^4) + 20\tilde{b}^3(5+6\tilde{z})\right.\\ &+ 24\tilde{b}^2\tilde{z}(5+6\tilde{z}) + 32\tilde{b}\tilde{z}^2(5+6\tilde{z}) + 64\tilde{z}^3(5+6\tilde{z}) + 20\tilde{a}^3(5+3\tilde{b}+6\tilde{z})\\ &+ 6\tilde{a}^2(9\tilde{b}^2 + 2\tilde{b}(5+6\tilde{z}) + 4\tilde{z}(5+6\tilde{z})) + 4\tilde{a}(15\tilde{b}^3 + 3\tilde{b}^2(5+6\tilde{z})\\ &\left.+ 4\tilde{b}\tilde{z}(5+6\tilde{z}) + 8\tilde{z}^2(5+6\tilde{z}))\}\right]\end{aligned} \tag{100}$$

where $\tilde{A} = A\lambda^5$. Because $\tilde{H}(\tilde{z})$ should behave like $\tilde{z}^{-1}$ for $\tilde{z} \to \infty$, so using (100) and also (34) and (35), one can arrive at

$$\frac{1}{16}\tilde{A}\,[5(8\tilde{\sigma}^4 + 24\tilde{\sigma}^2\tilde{\tau}^2 + 3\tilde{\tau}^4) + 6\tilde{\sigma}\,(8\tilde{\sigma}^4 + 40\tilde{\sigma}^2\tilde{\tau}^2 + 15\tilde{\tau}^4)] = 0 \tag{101}$$

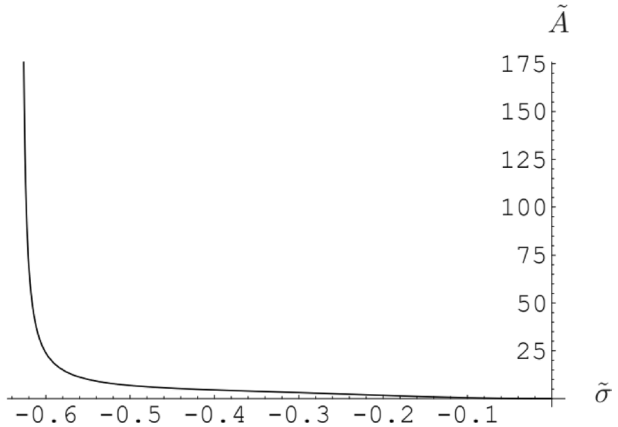

Figure 16. Surface area for $G(z) = z^4 + \lambda z$.

$$\frac{5}{16}\tilde{\tau}^2\left[4(4\tilde{\sigma}^3+3\tilde{\sigma}\,\tilde{\tau}^2)+3(8\tilde{\sigma}^4+12\tilde{\sigma}^2\tilde{\tau}^2+\tilde{\tau}^4)\right]=\frac{1}{\tilde{A}}. \tag{102}$$

The last two equations, lead to

$$\tilde{\tau}^2=-\frac{2\left(30\tilde{\sigma}^2+60\tilde{\sigma}^3+\sqrt{30}\sqrt{\tilde{\sigma}^4(25+84\tilde{\sigma}+84\tilde{\sigma}^2)}\right)}{15(1+6\tilde{\sigma})}, \tag{103}$$

$$\begin{aligned}\tilde{A}=&[15(1+6\tilde{\sigma})^3]/[\tilde{\sigma}\left(30\tilde{\sigma}^2+60\tilde{\sigma}^3+\sqrt{30}\sqrt{\tilde{\sigma}^4(25+84\tilde{\sigma}+84\tilde{\sigma}^2)}\right)\{20\tilde{\sigma}^2\\&+14\tilde{\sigma}^2\left(24\tilde{\sigma}^3+\sqrt{30}\sqrt{\tilde{\sigma}^4(25+84\tilde{\sigma}+84\tilde{\sigma}^2)}\right)+\left(140\tilde{\sigma}^3+\sqrt{30}\sqrt{\tilde{\sigma}^4(25+84\tilde{\sigma}+84\tilde{\sigma}^2)}\right)\\&+7\left(48\tilde{\sigma}^4+\sqrt{30}\tilde{\sigma}\sqrt{\tilde{\sigma}^4(25+84\tilde{\sigma}+84\tilde{\sigma}^2)}\right)\}].\end{aligned} \tag{104}$$

Using these two equations and the condition $\tilde{\tau}^2\geq 0$, and also using the fact that $\tilde{\tau}$ and $\tilde{A}$ should not be infinity, the following condition is obtained

$$-0.8333<\tilde{\sigma}<0. \tag{105}$$

Now, by using (104), one can plot $\tilde{A}$ as a function of $\tilde{\sigma}$ on the interval (105) as shown in Fig. 17. It is seen that this figure is similar to Fig. 13 for $T<T_c$.

In the same way as before, if one considers

$$G(z)=z^6+\lambda z^4, \tag{106}$$

by rescaling $\tilde{z}=z/\sqrt{\lambda}$ and doing some calculations, one can get $\tilde{\tau}^2<0$ for all $\tilde{\sigma}$. Thus, this model has not real answers.

If

$$G(z)=z^6+\lambda z^3, \tag{107}$$

by rescaling $\tilde{z}=\frac{z}{\lambda^{1/3}}$ and using the condition $\tilde{\tau}^2\geq 0$, one has

$$\begin{aligned}\tilde{A}=&-(1800\tilde{\sigma}^3)/[\left(1+20\tilde{\sigma}^3+\sqrt{1-20\tilde{\sigma}^3+280\tilde{\sigma}^6}\right)\{1-70\tilde{\sigma}^3\\&\times\left(8\tilde{\sigma}^3+\sqrt{1-20\tilde{\sigma}^3+280\tilde{\sigma}^6}\right)+\left(100\tilde{\sigma}^3+\sqrt{1-20\tilde{\sigma}^3+280\tilde{\sigma}^6}\right)\}],\end{aligned} \tag{108}$$

and

$$-0.793701<\tilde{\sigma}<0. \tag{109}$$

By plotting $\tilde{A}$ as a function of $\tilde{\sigma}$ as shown in Fig. 18, it is seen that the figure is similar to Fig. 13 for $T<T_c$.

Now, if one considers

$$G(z)=z^6+\lambda z^2, \tag{110}$$

by rescaling $\tilde{z}=\frac{z}{\lambda^{1/4}}$ and doing some calculations, it is seen that $\tilde{\tau}^2<0$ for all $\tilde{\sigma}$. Thus, there is no reall answer for this model.

Finally, by considering

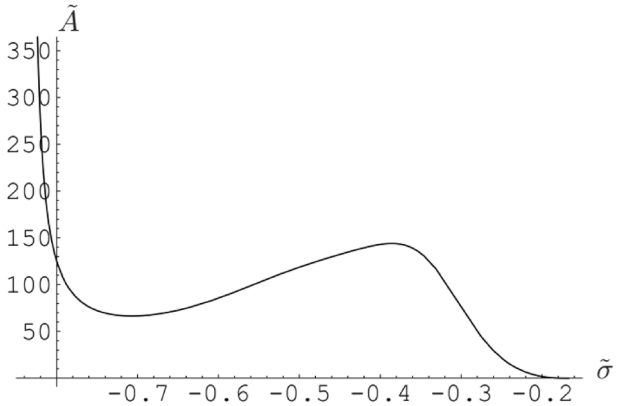

Figure 17. Surface area for $G(z)=z^6+\lambda z^5$.

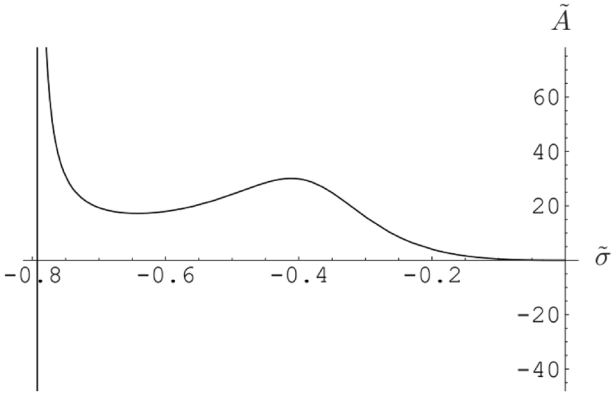

Figure 18. Surface area for $G(z) = z^6 + \lambda z^3$.

$$G(z) = z^6 + \lambda z, \tag{111}$$

and rescaling $\tilde{z} = \frac{z}{\lambda^{1/5}}$ and also doing the calculations mentioned earlier, one can obtain

$$\tilde{A} = (90\tilde{\sigma}^2)/[\left(10\tilde{\sigma}^3 + \sqrt{-5\tilde{\sigma} + 70\tilde{\sigma}^6}\right)\left(1 + 14\tilde{\sigma}^2\left(4\tilde{\sigma}^3 + \sqrt{-5\tilde{\sigma} + 70\tilde{\sigma}^6}\right)\right)], \tag{112}$$

and

$$-0.698827 < \tilde{\sigma} < 0. \tag{113}$$

Now, one can plot $\tilde{A}$ as a function of $\tilde{\sigma}$ as shown in Fig. 19 and see that this figure is similar to Fig. 13 for $T > T_c$.

As a result, as seen in the previous section, the model $G(z)$ plays the role of the temperature and so by using an appropriate model in two-dimensional space-time, one can describe a physical event in four-dimensional space-time.

Concluding remarks

First, a gYM_2 on the sphere with quartic and cubic couplings was studied. The effect of the cubic coupling on the density and the free energy was investigated. It was seen that there were four subintervals that in two of which the density was not nonnegative, which should be nonnegative, and so had to be redefined. Redefining the density, the free energy experienced two phase transitions one of which was of third order, like previous papers, and the other one was of second order, which is a novel result. Second, gYM_2 for $G(z) = z^4 + \lambda z^n (n < 4)$ and Maxwell construction were compared with each other and it was seen that there was a relationship between two-dimensional space-time and four-dimensional space-time. In the end, the models $G(z) = z^6 + \lambda z^n (n < 6)$ were studied and by comparing with Maxwell construction the equivalent parameters in two-dimensional space-time and Maxwell construction such as pressure, temperature and volume were found. This comparison is completety new and there is not like this in other papers. As a result, this paper can be a starting point for finding more relationships between two-dimensional and four-dimensional space-time to describe physical events accurately.

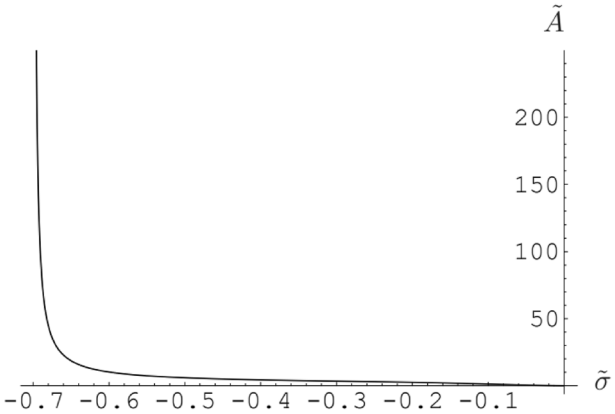

Figure 19. Surface area for $G(z) = z^6 + \lambda z$.

Data availability

The datasets used and/or analyzed during the current study available from the corresponding author on reasonable request.

Received: 6 January 2024; Accepted: 6 August 2024
Published online: 12 August 2024

References

1. Witten, E. Two dimensional gauge theories revisited. *J. Geom. Phys.* **9**, 303–368 (1992).
2. Witten, E. On quantum gauge theories in two dimensions. *Commun. Math. Phys.* **141**, 153–209 (1991).
3. Tan, S. G., Jalil, M. B., Ho, C. S., Siu, Z. & Murakami, S. Gauge physics of spin Hall effect. *Sci. Rep.* **5**, 18409 (2015).
4. Britto, R., Cachazo, F., Feng, B. & Witten, E. Direct proof of the tree-level scattering amplitude recursion relation in Yang–Mills theory. *Phys. Rev. Lett.* **94**, 181602 (2005).
5. Zhang, Xinyu. Partition function of N = 2 supersymmetric gauge theory and two-dimensional Yang–Mills theory. *Phys. Rev. D* **96**, 025008 (2017).
6. Hall, B. C. The large-N limit for two-dimensional Yang–Mills theory. *Commun. Math. Phys.* **363**, 789–828 (2018).
7. Binder, D. J., Chester, S. M., Pufu, S. S. & Wang, Y. N = 4 Super–Yang–Mills correlators at strong coupling from string theory and localization. *J. High Energy Phys.* **12**, 119 (2019).
8. Iraso, R. & Mney, P. Two-dimensional Yang–Mills theory on surfaces with corners in Batalin–Vilkovisky -Formalism. *Commun. Math. Phys.* **370**, 637–702 (2019).
9. Chester, S. M., Green, M. B., Pufu, S. S. & Wang, Y. New modular invariants in N = 4 Super-Yang-Mills theory. *J. High Energy Phys.* **04**, 212 (2021).
10. Fukuma, M., Kadoh, D. & Matsumoto, N. Tensor network approach to two-dimensional Yang-Mills theories. *Progress Theor. Exp. Phys.* **2021**, 123B03 (2021).
11. Monteiro, Ricardo, Stark-Muchão, Ricardo & Wikeley, Sam. Anomaly and double copy in quantum self-dual Yang–Mills and gravity. *J. High Energy Phys.* **09**, 030 (2023).
12. Bringmann B & Cao, S. A para-controlled approach to the stochastic Yang–Mills equation in two dimensions. arXiv:2305.07197 (2023).
13. Fine, D. Quantum Yang–Mills on the two-sphere. *Commun. Math. Phys.* **134**, 273–292 (1990).
14. Gross, D. J. Two-dimensional QCD as a string theory. *Nucl. Phys. B* **400**, 161–180 (1993).
15. Blau, M. & Thompson, G. Quantum Yang–Mills theory on arbitrary surfaces. *Int. J. Mod. Phys. A* **7**, 3781–3806 (1992).
16. Gross, D. J. & Taylor, W. Two-dimensional QCD is a string theory. *Nucl. Phys. B* **400**, 181–208 (1993).
17. Gross, D. J. & Taylor, W. Twists and Wilson loops in the string theory of two-dimensional QCD. *Nucl. Phys. B* **403**, 395–449 (1993).
18. Douglas, M. R., Lie, K. & Staudacher, M. Generalized two-dimensional QCD. *Nucl. Phys. B* **420**, 118–140 (1994).
19. Ganor, O., Sonnenschein, J. & Yankielowicz, S. The string theory approach to generalized 2D Yang–Mills theory. *Nucl. Phys. B* **434**, 139–178 (1995).
20. Khorrami, M. & Alimohammadi, M. Observables of the generalized 2D Yang–Mills theories on arbitrary surfaces: A path integral approach. *Mod. Phys. Lett. A* **12**, 2265–2270 (1997).
21. Alimohammadi, M. & Khorrami, M. n-Point functions of 2d Yang–Mills theories on Riemann surfaces. *Int. J. Mod. Phys. A* **12**, 1959–1965 (1997).
22. Alimohammadi, M. & Khorrami, M. Greens functions of 2-dimensional Yang–Mills theories on nonorientable surfaces. *Z. Phys. C* **76**, 729–731 (1997).
23. Douglas, M. R. & Kazakov, V. A. Large N phase transition in continuum QCD_2. *Phys. Lett. B* **319**, 219–230 (1993).
24. Minahan, J. A. & Polychronakos, A. P. Equivalence of two-dimensional QCD and the c = 1 matrix model. *Phys. Lett. B* **312**, 155–165 (1993).
25. Minahan, J. A. & Polychronakos, A. P. Classical solutions for two-dimensional QCD on the sphere. *Nucl. Phys. B* **422**, 172–194 (1994).
26. Aghamohammadi, A., Alimohammadi, M. & Khorrami, M. Uniqueness of the minimum of the free energy of the 2-D Yang–Mills theory at large N. *Mod. Phys. Lett. A* **14**, 751–758 (1999).
27. Rusakov, B. & Yankielowicz, S. Large N phase transitions and multi-critical behaviour in generalized 2D QCD. *Phys. Lett. B* **339**, 258–262 (1994).
28. Alimohammadi, M., Khorrami, M. & Aghamohammadi, A. Large-N limit of the generalized two-dimensional Yang–Mills theories. *Nucl. Phys. B* **510**, 313–323 (1998).
29. Rusakov, B. Large-N quantum gauge theories in two dimensions. *Phys. Lett. B* **303**, 95–98 (1993).
30. Gross, D. J. & Witten, E. Possible third-order phase transition in the large-N lattice gauge theory. *Phys. Rev. D* **21**, 446 (1980).
31. Alimohammadi, M. & Tofighi, A. Phase structure of the generalized two-dimensional Yang–Mills theory on sphere. *Eur. Phys. J. C* **8**, 711–717 (1999).
32. Lavaei-Yanesi, L. & Khorrami, M. Phase structure of the quartic-cubic generalized two dimensional Yang–Mills U(N) on the sphere. *Math. Phys.* **49**, 073514 (2008).
33. Popov, V. S. & Perelomov, A. M. A generating function for Casimir operators. *Sov. Math. Dokl.* **8**, 712 (1967).
34. Brezin, E., Itzykson, C., Parisi, G. & Zuber, J. B. Planar diagrams. *Commun. Math. Phys.* **59**, 35–51 (1978).
35. Huang, K. *Statistical Mechanics*, 2nd edition, chapter 2 (Wiley, 1987).

Acknowledgements

I would like to thank Mohammad Khorrami for useful discussions.

Author contributions

L. L prepared the whole of this paper alone.

Competing interests

The author declares no competing interests.

Additional information

Correspondence and requests for materials should be addressed to L.L.

Reprints and permissions information is available at www.nature.com/reprints.